ANTIMICROBIAL AGENTS AND CHEMOTHERAPY, Mar. 2001, p. 679–685 Vol. 45, No. 3
0066-4804/01/$04.00+0 DOI: 10.1128/AAC.45.3.679–685.2001

Apoptosis Contributes to Amphotericin B-Induced Nephrotoxicity

DESPINA E. VARLAM,[1]† MUSTAFA M. SIDDIQ,[1] LANCE A. PARTON,[1]‡ AND HOLGER RÜSSMANN[2]*

Department of Pediatrics, SUNY at Stony Brook, Stony Brook, New York 11794-8111,[1] and Max von Pettenkofer-Institute for Hygiene and Medical Microbiology, Ludwig Maximilians University, 80336 Munich, Germany[2]

Received 8 September 2000/Returned for modification 17 October 2000/Accepted 5 December 2000

The aim of this study was to investigate whether apoptosis contributes to nephrotoxicity caused by amphotericin B (AmB). By detecting apoptosis-specific DNA fragmentation, it is demonstrated that proximal tubular cells (LLC-PK_1) and medullary interstitial cells (RMIC) respond with programmed cell death when treated with therapeutic doses of AmB. Concomitant application of AmB and recombinant human insulin-like growth factor-1 (rhIGF-1), a known antiapoptotic agent, abrogated apoptosis in vitro. To validate that the observed apoptotic effects on renal tissue culture cells are applicable to an in vivo setting, an animal model was used for verification. Therefore, Sprague-Dawley rats were treated with AmB. The drug caused hypokalemia, decreased weight gain, loss of renal concentrating ability, and dehydration in a dose-dependent fashion. Microscopic examination of renal tissue sections revealed apoptotic alterations predominantly in proximal and distal tubular epithelial cells. To verify that the observed clinical side effects were linked to apoptosis, rhIGF-1 was applied concomitantly with AmB. In all animals, rhIGF-1 prevented the above-mentioned clinical side effects. Moreover, significantly reduced apoptosis was observed in renal tissue sections of these animals, indicating the relevance of apoptosis in nephrotoxicity. This is the first report to demonstrate that AmB induces apoptosis in the rat kidney in a dose-dependent fashion. The incidence of apoptosis correlates with renal toxicity and can be abrogated by concomitant treatment with rhIGF-1.

The polyene macrolide amphotericin B (AmB) has remained the drug of choice in fighting systemic fungal infections for more than 30 years. However, its toxic effects, particularly nephrotoxicity, remain a serious and dose-limiting side effect of therapy (16). In pediatrics, premature neonates are at high risk for systemic fungal infections. In addition, this group of patients is particularly susceptible to renal cell injury. Despite careful monitoring, treatment of this life-threatening infection frequently cannot be completed secondary to severe drug-induced renal side effects. AmB is known to cause hypokalemia, vasopressin-resistant polyuria, and uremia (5, 6). However, the cell-morphological alterations in kidneys causing these adverse effects are not yet fully understood.

The aim of this study was to identify the mechanism of AmB-mediated renal injury in vitro and to confirm the obtained results in vivo. Nephrotoxic agents can cause apoptosis and/or necrosis (42). In contrast to necrosis, which is associated with irreversible tissue damage, apoptosis is a physiological form of cell death with distinct biochemical features (17). Apoptotic cells are removed by macrophages, and there is no permanent loss of function of the affected tissue, whereas necrosis generates an inflammatory response resulting in the loss of tissue function (17). Since the clinical side effects of AmB are reversible after the discontinuation of therapy (16), it is tempting to speculate that AmB nephrotoxicity is mediated by apoptotic cell death.

In the present study, we investigated the influence of AmB and the known antiapoptotic agent recombinant human insulin-like growth factor-1 (rhIGF-1) on (i) renal tissue culture cell lines and (ii) in vivo in the rat model. Our results clearly demonstrate that AmB induces apoptosis in particular renal cell lines in a dose-dependent fashion. Moreover, the known clinical adverse effects of AmB correlate with the incidence of apoptosis in the rat kidney. In addition, we found that rhIGF-1 ameliorates AmB-induced side effects by preventing apoptosis in the rat kidney.

MATERIALS AND METHODS

Tissue culture cell lines. Passages four to seven of porcine proximal tubular cells (LLC-PK_1), canine distal tubular cells (MDCK), rat medullary interstitial cells (RMIC), and rat mesangial cells (ARMC) were used to investigate the cytotoxic effects of AmB. Cells were grown in Dulbecco modified Eagle medium (DMEM) (Life Technologies, Karlsruhe, Germany) supplemented with 10% heat-inactivated fetal bovine serum. Confluent cell monolayers were exposed in 96-well plates to AmB at concentrations of 0.5, 1.0, 2.5, or 5.0 μg/ml corresponding to renal tissue concentrations obtained from patients treated for invasive fungal infection (8). For 1 h, cells were exposed to AmB in DMEM without serum to prevent binding of the drug to serum albumin. After completion of this treatment, AmB was removed and cells were rinsed three times with phosphate-buffered saline (PBS) (Life Technologies).

In another set of experiments, cells were pretreated with 50 or 100 μg of rhIGF-1 (Genentech, Inc., South San Francisco, Calif.) per liter in DMEM without serum for 12 h prior to the exposure to AmB. Before AmB was added, cells were thoroughly rinsed three times with PBS.

Determination of cell death in renal tissue culture cell lines. Cell viability was determined by trypan blue exclusion at each time point. In contrast to apoptosis, necrosis results from a severe cellular insult in which internal organelle and plasma membrane integrity are lost (17, 38). Thus, necrotic cells were identified by uptake of the dye trypan blue. Qualitative measurement of apoptotic cells was carried out immunohistochemically by labeling DNA strand breaks with biotinylated nucleotides (14) and subsequent incubation with a streptavidin-horserad-

* Corresponding author. Mailing address: Max von Pettenkofer-Institute for Hygiene and Medical Microbiology, Ludwig Maximilians University, Pettenkoferstr. 9a, 80336 Munich, Germany. Phone: 0049-89-51605261. Fax: 0049-89-51605223. E-mail: ruessmann@m3401.mpk.med.uni-muenchen.de.

† Present address: Children's Hospital, Technical University, 80804 Munich, Germany.

‡ Present address: New York Medical College, Valhalla, NY 10595.

ish peroxidase conjugate according to the protocol provided by the manufacturer (In Situ Cell Death Detection Kit; TUNEL [terminal deoxynucleotidyl transferase-mediated dUTP-biotin nick end labeling] assay; Boehringer-Mannheim, Indianapolis, Ind.). Apoptotic nuclei stained dark blue. Analysis and quantification of apoptotic nuclei were carried out by light microscopy in a blinded fashion by two independent researchers. To determine the apoptotic and necrotic index in renal tissue culture cell lines, 100 cells were counted in 10 fields until a total of 1,000 cells had been reached. Each set of experiments was repeated three times. The results represent the cumulative means of all three experiments.

To substantiate the results, cytoplasmic histone-associated DNA fragments typical for apoptosis were determined by photometric enzyme immunoassay according to the protocol provided by the manufacturer (Cell Death Detection ELISA^{PLUS}; Boehringer-Mannheim). Briefly, cells were grown in 96-well microtiter plates and incubated with various doses of AmB and/or rhIGF−1. Subsequently, cells were lysed and centrifuged, and the supernatant containing the cytoplasmic fraction was transferred into streptavidin-coated microtiter plates. A mixture of anti-histone-biotin and anti-DNA-peroxidase was then added, and the samples were analyzed spectrophotometrically at 405 nm. An enzyme-linked immunosorbent assay (ELISA)-specific enrichment factor was used to calculate absorbance values as a percentage of apoptotic cells in the treatment groups compared to the control groups. Each experiment was performed in duplicate and repeated six times.

In order to verify that the observed AmB-induced cellular changes were indeed due to apoptosis, in another set of experiments 100 μmol of caspase-3 inhibitor (Oncogene Research, Boston, Mass.) was added per well to the AmB incubation media. After coincubation of AmB and caspase-3 inhibitor, the above-mentioned ELISA was performed.

Animals. Three-week-old male Sprague-Dawley rats weighing 80 to 100 g were held in individual cages with a constant 12-h light–12-h dark cycle. The animals had free access to a standard diet (Ralston-Purina Co., St. Louis, Mo.) and received water ad libitum. Prior to the beginning of the experiments, the rats were randomized and divided into eight groups consisting of 5 or 10 animals each. Animals of three experimental groups received conventional AmB intraperitoneally (i.p.) at 5 mg/kg/day (low dose), 10 mg/kg/day (medium dose), or 15 mg/kg/day (high dose). In addition to the application of AmB, three other groups received rhIGF-1 subcutaneously (s.c.) at 4 mg/kg/day. AmB was injected once daily on five consecutive days. The doses of AmB (20, 21). and rhIGF-1 (22, 23) were obtained in consultation with the literature. Like AmB, rhIGF-1 was given on five consecutive days, but the dosage was divided into two daily injections in order to avoid hypoglycemia. Another two experimental animal groups served as negative controls. These rats received either 5% glucose s.c. or rhIGF-1 s.c. at 4 mg/kg/day.

Measurement of body weight. Rats were weighed daily. Daily changes of body weight were determined at the same time every morning as the weight loss or gain in percent body weight compared to the weight of the previous day. The mean values of all five treatment days and the presacrifice weight on day six were determined.

Assessment of renal function. On day 5, rats were placed in individual metabolic cages for 24 h and had their urinary volume measured and urinary samples collected to assess the urine specific gravity. Serum potassium, sodium, blood urea nitrogen (BUN), and creatinine levels were measured by standardized autoanalyzer methods. Blood was obtained by central venous catheterization of the external jugular vein after anesthesia with pentobarbital (45 mg/kg).

Histology. Kidneys were embedded in paraffin, and 4-μm tissue sections were prepared. (i) Apoptotic cells were detected immunohistochemically in tissue sections of the kidney by using the In Situ Cell Death Detection Kit (TUNEL assay; Boehringer-Mannheim). Briefly, fixed renal tissue sections were deparaffinized and rehydrated in ethanol. Samples were incubated with proteinase K (Sigma) and subsequently with terminal dideoxynucleotidyl transferase, which was used to incorporate hapten-tagged nucleotides into the 3′-DNA strand breaks that occur during apoptosis. This specific labeling technique stains the apoptotic nuclei dark blue. To further verify the results, apoptotic cells were also identified by detecting phosphatidylserine (PS) on the outer plasma membrane leaflet (Annexin V Staining Kit; Boehringer Mannheim). In early stages of apoptosis, PS is translocated from the inner part to the outer layer of the plasma membrane. Annexin V, a Ca^{2+}-dependent phospholipid-binding protein, possesses high affinity for PS, thus recognizing specifically early apoptotic cells. (ii) Necrotic cells were excluded by trypan blue staining. In contrast to apoptotic cells, the cell membrane of necrotic cells is disrupted. Thus, the dye trypan blue can invade the necrotic cell and stain the cytoplasma blue.

Analysis and quantification of apoptotic and necrotic cells were carried out by light microscopy in a blinded fashion by two independent researchers. To determine the apoptotic and necrotic index of mesangial cells in tissue sections, the number of apoptotic and necrotic cells within 50 glomeruli was counted and divided by the total number of mesangial cells within these glomeruli. The apoptotic and necrotic index values within the tubulointerstitium of each tissue section were calculated by counting the total number of positive cells in 30 sequentially selected 0.5-mm^2 grids at a ×100 magnification.

Statistical analysis. One-way analysis of variance with the Bonferroni correction was performed to analyze the data obtained in this study. A P value of <0.05 was considered to reflect statistically significant data. Graphs represent the mean ± 1 standard deviation.

RESULTS

Determination of cytotoxic effects in renal tissue culture cell lines. (i) AmB application. In this study, renal tissue culture cell lines, i.e., rat mesangial cells (ARMC), canine distal tubular cells (MDCK), rat medullary interstitial cells (RMIC), and porcine proximal tubular cells (LLC-PK_1) representing four physiologically relevant units of the nephron were used to investigate the cytotoxic effects of AmB on the kidney. These cell lines were exposed to AmB at concentrations of 0, 0.5, 1.0, 2.5, or 5.0 μg/ml for 1 h. Subsequently, apoptotic cells were detected immunohistochemically by the end labeling of DNA strand breaks (TUNEL assay) or necrotic cells by the trypan blue exclusion assay.

As shown in Fig. 1, all untreated cell lines revealed an apoptotic and necrotic index value of <1%. In contrast, a high necrotic index (<90%) was determined in all cell lines incubated with 5.0 μg of AmB per ml.

ARMC exposed to AmB showed no significant signs of apoptosis. Treatment of MDCK with 2.5 μg of AmB per ml resulted in a significant increase of apoptotic cells (8% ± 1%, $P < 0.05$) compared to untreated control cells. In a dose-dependent fashion, marked apoptotic effects (49% ± 5% to 93% ± 6%) were observed in RMIC and LLC-PK_1 incubated with 1 or 2.5 μg of AmB per ml.

To confirm that the toxic cell alterations induced by AmB are due to apoptosis, histone-associated DNA fragmentation, which is characteristic of this type of cell death, was measured by ELISA. To further underpin that the observed cell death is due to apoptosis rather than indiscriminate DNA digestion, a caspase-3 inhibitor was used to specifically block the apoptotic pathway prior to performing the above-mentioned ELISA.

Table 1 reveals that the determination of apoptosis by measuring histone-associated DNA fragmentation using LLC-PK_1 exposed to AmB gave concordant results compared to the results derived from the TUNEL staining (Fig. 1). The dose-dependent induction of apoptosis by AmB was completely blocked by the application of 100 μmol of caspase-3 inhibitor (Table 1). Cytosolic aspartate-specific proteases, called caspases, are responsible for the deliberate disassembly of a cell into apoptotic bodies. Caspase-3 is situated at a pivotal junction in the apoptotic pathway (35, 36). Therefore, by inhibiting caspase-3 the cell becomes unable to undergo apoptosis, and cellular damage would be due to indiscriminate DNA fragmentation rather than to specific apoptotic cell death.

(ii) Concomitant application of AmB and rhIGF-1. It has been demonstrated in several reports that IGF-1 prevents apoptotic cell death in neuronal cells (3, 10, 26, 35), as well as in cardiac fibroblasts (28). In the kidney, IGF-1 was found to accelarate recovery in renal failure (18) and to improve the acute nephrotoxic effects of cyclosporine (24). Since our results show so far that AmB does not cause significant apoptosis in

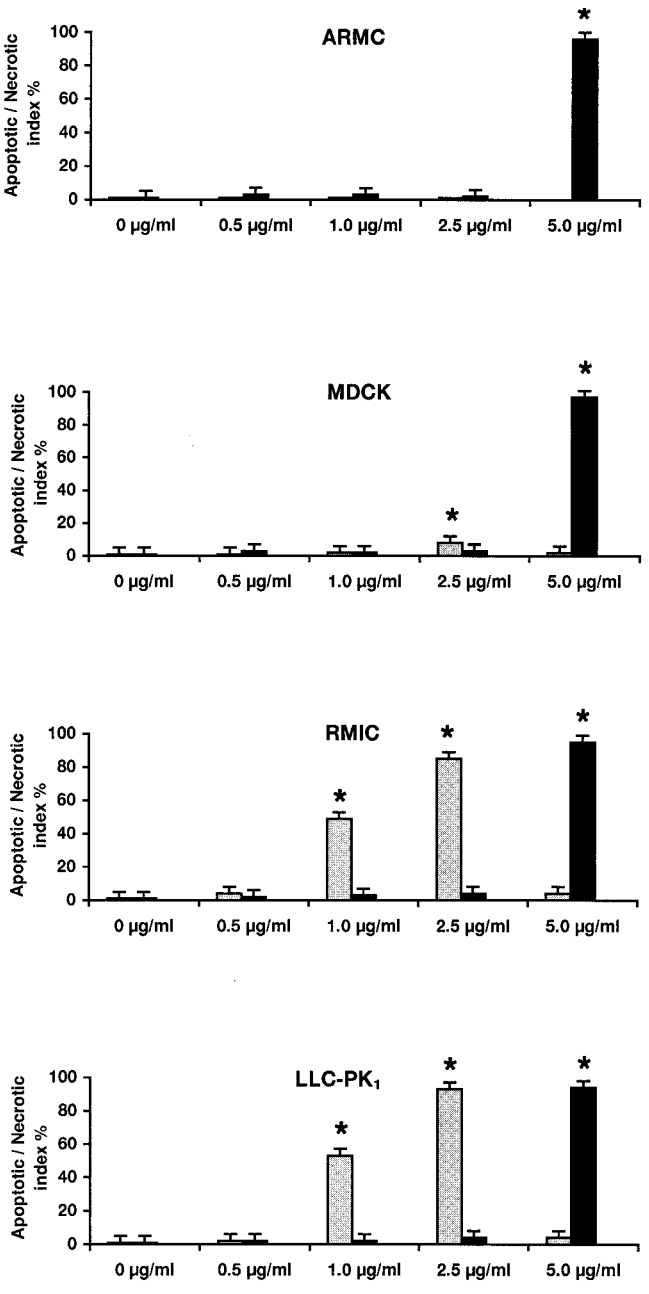

FIG. 1. Determination of the apoptotic (gray columns) and necrotic (black columns) index values in renal tissue culture cell lines after application of AmB. Confluent monolayers of rat mesangial cells (ARMC), canine distal tubular cells (MDCK), rat medullary interstitial cells (RMIC), and porcine proximal tubular cells (LLC-PK_1) were exposed to various AmB concentrations. Apoptotic cells were detected immunohistochemically by end labeling of DNA strand breaks (TUNEL assay) or necrotic cells by the trypan blue exclusion assay, respectively. Each set of experiments was repeated three times. The columns represent the means of results from all four experiments. Standard deviations of the means are indicated by error bars. *, Value differs significantly from that of untreated control groups ($P < 0.05$).

mesangial cells and since mesangial cells are known to be the only cells of the kidney to produce IGF-1 intrinsically (2, 9, 34), we hypothesize that IGF-1 might elicit a protective effect in toxic renal injury. Therefore, in a next set of experiments, we investigated whether the preincubation of renal tissue culture cell lines with rhIGF-1 prior to the application of AmB reduces apoptosis. Table 2 reveals that RMIC, as well as LLC-PK_1, showed a significant rhIGF-1 dose-dependent reduction of AmB-induced apoptosis.

To demonstrate that the observed apoptotic effects on renal tissue culture cells are applicable to an in vivo setting, we used a rat model for verification. Therefore, in the second part of the study Sprague-Dawley rats were treated with AmB alone or in combination with rhIGF-1.

Determination of clinical side effects in rats. (i) AmB application. As shown in Table 3, Sprague-Dawley rats were given various doses of AmB on five consecutive days, whereas animals of negative control groups did not receive AmB. Rats treated with 5 or 10 mg of AmB/kg/day gained significantly less weight than animals of both control groups. Moreover, rats treated with 15 mg/kg/day lost 10% ±2% of their body weight daily.

Potassium levels in serum were obtained by careful blood sampling from a central venous catheter which was placed in the external jugular vein. Statistical analysis of all three AmB treatment groups revealed a significant decrease of potassium levels in animals which had received AmB at 10 or 15 mg/kg/day compared to the control groups.

The urinary concentrating ability of individual rats was determined by measuring the urinary specific gravity in 24-h-collected urine specimens on the last treatment day. The urinary specific gravity was significantly lower in all three AmB treatment groups compared to the control groups.

Further assessment of renal function as reflected by serum creatinine levels and BUN measurements did not show a significant difference between all experimental groups (data not shown). Serum creatinine levels ranged from 0.1 to 0.2 mg/dl in all animals (normal range for 3-week-old rats, 0.1 to 0.3 mg/dl). Also, all rats could preserve their serum sodium concentration.

Taken together, in the rat model AmB causes hypokalemia and dehydration as reflected by decreased weight gain and the loss of renal concentrating ability, which are well known clinical side effects of AmB treatment in humans.

(ii) Concomitant application of AmB and rhIGF-1. As shown in Table 3, Sprague-Dawley rats belonging to three experimental groups were given rhIGF-1 in addition to various doses of AmB. All animals concomitantly treated with both drugs gained more weight than rats treated with AmB alone. Moreover, Table 3 reveals that in animals which had received 10 or 15 mg of AmB/kg/day in combination with rhIGF-1, serum potassium levels were significantly higher compared to rats treated with AmB alone. The measurement of the urine specific gravity showed that the urinary concentrating ability was preserved in all animals which had received AmB together with rhIGF-1.

In summary, rhIGF-1 prevents hypokalemia and dehydration in rats when applied concomitantly with AmB.

Histopathological examination of rat kidneys. Following sacrifice of the rats, renal tissue sections were prepared to detect apoptotic and necrotic cells by light microscopy. Quantification of cell damage is reflected by the apoptotic and necrotic index values as described above.

(i) AmB application. In Table 3, it is demonstrated that the determination of the necrotic index by trypan blue exclusion

TABLE 1. Quantitative measurement of histone-associated DNA fragmentation in monolayers of porcine proximal tubular cells (LLC-PK_1) by photometric ELISA

Drug application group[a]	% DNA fragmentation[b] ± SD
No AmB	1.0 ± 0.34
No AmB plus 100 μmol of caspase-3 inhibitor	0.8 ± 0.23
AmB (0.5 μg/ml)	22.0 ± 0.35*
AmB (0.5 μg/ml) plus 100 μmol of caspase-3 inhibitor	1.5 ± 0.26
AmB (1.0 μg/ml)	41.0 ± 1.36*
AmB (1.0 μg/ml) plus 100 μmol of caspase-3 inhibitor	1.0 ± 0.26
AmB (2.5 μg/ml)	80.0 ± 3.25*
AmB (2.5 μg/ml) plus 100 μmol of caspase-3 inhibitor	1.0 ± 0.41

[a] LLC-PK_1 were exposed to no AmB, AmB alone, or in combination with caspase-3 inhibitor as indicated.
[b] Values are the means ± the standard deviation of data from duplicates of seven independent experiments. *, Value differs significantly from that of the untreated control group (no AmB) ($P < 0.05$).

TABLE 2. Determination of the AI of rat medullary interstitial cells (RMIC) and porcine proximal tubular cells (LLC-PK_1) by end-labeling of DNA strand breaks (TUNEL assay)

Drug application group[a]	AI[b] (mean % ± SD)	
	RMIC	LLC-PK_1
AmB (1.0 μg/ml)	49 ± 5	53 ± 4
AmB (1.0 μg/ml) plus 50 μg of rhIGF-1 per liter	25 ± 5*	23 ± 5*
AmB (1.0 μg/ml) plus 100 μg of rhIGF-1 per liter	5 ± 1*	3 ± 1*
AmB (2.5 μg/ml)	85 ± 9	93 ± 6
AmB (2.5 μg/ml) plus 50 μg of rhIGF-1 per liter	36 ± 6*	49 ± 4*
AmB (2.5 μg/ml) plus 100 μg of rhIGF-1 per liter	3 ± 1*	4 ± 2*

[a] RMIC and LLC-PK_1 were exposed to AmB alone or in combination with rhIGF-1 as indicated.
[b] Values are the means ± the standard deviation of data from four independent experiments. *, Value differs significantly from that of the drug application group AmB at 1.0 μg/ml or AmB at 2.5 μg/ml, respectively ($P < 0.05$).

unveiled 1% necrotic cells in renal tissue sections from rats which received 5 or 10 mg of AmB/kg/day. However, the application of 15 mg of AmB/kg/day resulted in a significant increase of necrosis in tubular epithelial and mesangial cells.

The comparison of both applied apoptosis detection techniques, i.e., TUNEL assay and Annexin V staining, revealed no statistically significant differences. As shown in Table 3, rats of both negative control groups revealed <4% apoptotic cells in kidney tissue. In contrast, the application of 5 mg of AmB/kg/day induced significant apoptosis in tubular epithelial cells (Fig. 2), whereas no such alterations were observed in mesangial cells In the experimental group treated with 10 mg of AmB/kg/day, significant apoptosis was observed in tubular epithelial cells (apoptotic index, 52% ± 6%). In addition, few apoptotic cells were detected within the mesangium (apoptotic index, 5% ± 2%). Animals which had received 15 mg of AmB/kg/day showed pronounced apoptosis in renal tubular epithelial cells and a significant increase in apoptosis in mesangial cells (Fig. 2).

(ii) Concomitant application of AmB and rhIGF-1. Table 3 reveals that rhIGF-1 prevented renal apoptosis in tubular epithelial cells in animals which were treated with AmB at 5 mg/kg/day (Fig. 2) and significantly reduced apoptosis in animals which had received AmB at 10 mg/kg/day or at 15 mg/kg/day. In mesangial cells, this protective effect of rhIG-1 was observed, too (Fig. 2).

Trypan blue exclusion did not reveal statistically significant differences regarding necrotic cells in experimental groups treated with 5 or 10 mg of AmB/kg/day. However, the necrotic index of tubular epithelial and mesangial cells of rats which had received 15 mg of AmB/kg/day was significantly reduced by concomitant application of rhIGF-1.

DISCUSSION

With advances in medicine, there is an increasing number of immunocompromised patients and premature neonates who are at risk for acquiring systemic fungal infections. AmB is widely used to fight invasive fungal infections (16, 25). AmB causes severe renal side effects (6, 41). Its nephrotoxicity is a limiting factor for the duration of therapy (32). In 1974, Weldon and Schultz documented that acute AmB nephrotoxicity in rats results in minor histological alterations, primarily mild swelling of the glomeruli and proximal as well as distal tubular epithelial cells (40). AmB nephrotoxicity during long-term treatment is known to be manifested by vasopressin-resistant polyuria and hypokalemia associated with a reduced creatinine clearance and tubular acidosis (15). These side effects are attributed primarily to increased renal vascular resistance and tubular permeability due to binding of AmB to cell membranes, formation of transmembrane pores, and leakage of electrolytes (4, 6). Further in vitro studies conducted by Joly et al. demonstrated an increased release of LDH into the supernatant of rabbit proximal tubular cells after incubation with AmB in nontherapeutic high concentrations exceeding 40 μg/ml (19). Increased LDH release is a marker of cell membrane disintegration and necrosis. Since AmB toxicity is reversible after discontinuation of the drug (32), we speculated that mechanisms other than necrosis are involved in its nephrotoxicity when AmB is administered in therapeutic dose ranges. Necrotic cells are unable to maintain homeostasis. The influx of water and ions lead to cell lysis, followed by a release of cytoplasmic content into the extracellular fluid resulting in an intense inflammatory response (38). Apoptosis, in contrast, is a mode of cell death which occurs under physiological conditions, and the cell is an active participant in its own demise (38). In vivo, apoptotic bodies are rapidly recognized and phagocytozed without loss of tissue function (38).

The aim of the present study was to evaluate the role of apoptosis in AmB-induced nephrotoxicity using various renal tissue culture cell lines and the rat model. By detecting apoptosis-specific DNA fragmentation, we could clearly demonstrate that proximal tubular cells (LLC-PK_1) and medullary interstitial cells (RMIC) respond with apoptosis in a dose-dependent fashion. In contrast, the apoptotic effect in distal tubular cells (MDCK) was significantly lower, and no apoptotic nuclei were observed following exposure of mesangial cells (ARMC) to AmB. In accordance with the work of Joly et al. (19), all four renal cell lines showed pronounced necrosis when treated with a supratherapeutic AmB concentration (5 μg/ml).

Nonspecific DNA fragmentation may mimic apoptosis. In this study, it was therefore important to detect apoptotic changes by several techniques using different markers. Cyto-

TABLE 3. Determination of clinical side effects and apoptotic and necrotic index values in renal tissue sections of rats treated with AmB[a]

Experimental group (route)[b]	Clinical side effects (mean % ± SD)			Renal tissue sections (mean % ± SD)					
				Tubular epithelial cells			Mesangial cells		
				AI[c]		Necrotic index[d]	AI[c]		Necrotic index[d]
	Daily % wt change ± SD	Serum potassium (mmol/liter ± SD)	Urine specific gravity	TUNEL	Annexin V		TUNEL	Annexin V	
5% glucose (s.c.)	+ 10 ± 1.0	4.5 ± 0.146	1.023 ± 0.002	3 ± 1	3 ± 1	2 ± 1	2 ± 1	2 ± 1	2 ± 1
rhIGF-1, 4 mg/kg/day (s.c.)	+ 12 ± 1.6	4.6 ± 0.146	1.025 ± 0.002	2 ± 1	2 ± 1	1 ± 1	1 ± 1	1 ± 1	1 ± 1
AmB, 5 mg/kg/day (i.p.)	+ 8 ± 0.7*	4.5 ± 0.146	1.020 ± 0.002*	43 ± 4*	42 ± 2*	1 ± 1	1 ± 1	1 ± 1	1 ± 1
AmB, 5 mg/kg/day (i.p.), plus rhIGF-1, 4 mg/kg/day (s.c.)	+ 10 ± 1.1	4.6 ± 0.241	1.025 ± 0.001	2 ± 1	3 ± 1	2 ± 1	1 ± 1	1 ± 1	1 ± 1
AmB, 10 mg/kg/day (i.p.)	+ 8 ± 0.3*	3.9 ± 0.146*	1.005 ± 0.002*	52 ± 6*	54 ± 4*	4 ± 2	5 ± 2*	4 ± 1*	2 ± 1
AmB, 10 mg/kg/day (i.p.), plus rhIGF-1, 4 mg/kg/day (s.c.)	+ 10 ± 1.0	4.5 ± 0.146	1.020 ± 0.003*	18 ± 2*	17 ± 2*	2 ± 1	2 ± 1	2 ± 1	1 ± 1
AmB, 15 mg/kg/day (i.p.)	− 10 ± 2.0*	2.9 ± 0.155*	1.001 ± 0.002*	92 ± 6*	91 ± 4*	10 ± 2*	25 ± 1*	24 ± 1*	4 ± 1*
AmB, 15 mg/kg/day (i.p.), plus rhIGF-1, 4 mg/kg/day (s.c.)	+ 8 ± 1.0*	4.4 ± 0.146	1.015 ± 0.001*	29 ± 1*	28 ± 2*	3 ± 1	5 ± 1*	6 ± 1*	1 ± 1

[a] *, Value differs significantly from that of experimental control groups (5% glucose [s.c.] or 4 mg of rhIGF-1/kg/day [s.c.]) ($P < 0.05$).
[b] Rats were treated with AmB alone or in combination with rhIGF-1 as indicated. Animals which received 5% glucose s.c. or rhIGF-1 s.c. at 4 mg/kg/day served as negative controls.
[c] Apoptotic cells were identified immunohistochemically by the detection of 3′-DNA strand breaks (TUNEL assay) and by staining of PS with Annexin V.
[d] Necrotic cells were identified by trypan blue staining.

solic aspartate-specific proteases, called caspases, are responsible for the deliberate disassembly of a cell into apoptotic bodies. Caspase-3 is situated at a pivotal junction in the apoptotic pathway (39). By inhibiting caspase-3, cells are unable to undergo apoptosis. In our experiments, apoptosis was completely blocked by caspase-3 inhibitor. This suggests that the AmB-induced cellular changes are specific for programmed cell death rather than indiscriminate toxicity.

In our experimental setup, the major injury reflected by the apoptotic index (AI) occurred in proximal tubular cells; nevertheless, some injury could also be detected in distal tubular cells. It is unclear why a higher AI is found in proximal tubular cells, since physiological potassium excretion occurs primarily in the distal tubules. Increased apoptosis in proximal tubular cells might be responsible for increased potassium secretion, thus exceeding the absorption threshold in the distal tubules which might be further compromised in the presence of apoptosis. Also, the AmB concentration in distal tubular cells in vivo might be much higher compared to the tissue culture cell situation because of the indirect effect of renal concentration mechanisms within the medulla. Interestingly, the apoptotic effect did not increase with repeated daily administration of 1 μg of AmB per ml (data not shown), which raises the possibility that the initial injury may be responsible for subsequent tubular damage. This hypothesis is supported by the work of Nouwen et al., who could demonstrate that in vivo injury to proximal tubules may alter gene expression in other areas of the kidney (29).

Nephrotoxic agents are able to induce apoptosis and/or necrosis to various degrees in other organs as well. The degree of cell damage depends on target cell- and toxic agent-specific activation of death mediators and/or survival factors that can lead to the common endpoint of apoptosis and/or necrosis. On one hand, renal cells are capable of producing intrinsic survival factors such as IGF-1, cyclooxygenase-2-derived prostaglandins, and eicosanoids, which facilitate recovery from (or prevent) toxic injury. (22). On the other hand, the antioxidative capacity of renal tubular epithelial cells is limited compared to, e.g., macrophages. It is conceivable that different cell types require different mediators to undergo apoptosis or to survive toxic injury. This might explain the differences of AmB concentration-dependent induction of apoptosis and necrosis between macrophages, renal mesangial cells, and tubular epithelial cells. Comparing the cytokine and growth factor profile of macrophages and tubular epithelial cells in response to toxic agents is of great interest and may help us to understand the organ specificity of drug toxicity.

In vitro, mesangial cells (ARMC) did not undergo apoptosis after AmB exposure. Since, on one hand, mesangial cells were reported to be the only cells of the kidney to produce IGF-1 (2, 9, 34) and, on the other hand, IGF-1 is a well known antiapoptotic agent (26, 28, 30, 33, 35), it is conceivable that intrinsically produced IGF-1 prevented apoptosis in ARMC. To investigate whether IGF-1 is able to elicit a nephroprotective effect, we exposed RMIC and LLC-PK_1 to 50 and 100 μg of rhIGF-1 per liter prior to the incubation with AmB. We found that rhIGF-1 significantly prevents apoptosis induced by AmB in interstitial and proximal tubular cells in vitro in a dose-dependent fashion.

The possibility that apoptosis may contribute to clinical adverse effects of AmB administration prompted us to address this issue in vivo. Therefore, in the second part of this study, we examined an experimental rat model of acute AmB nephrotoxicity with clinical side effects such as polyuria and hypokalemia similar to those induced by AmB in patients. Furthermore, we investigated whether acute side effects of AmB treatment could be ameliorated by preventing apoptosis with rhIGF-1.

We found that AmB induced apoptosis within renal tubular epithelial and interstitial cells of rat kidneys in a dose-dependent fashion. As in our in vitro findings, mesangial cells were not affected by apoptosis in rats receiving low and medium doses of AmB. However, a high dose of AmB caused a signif-

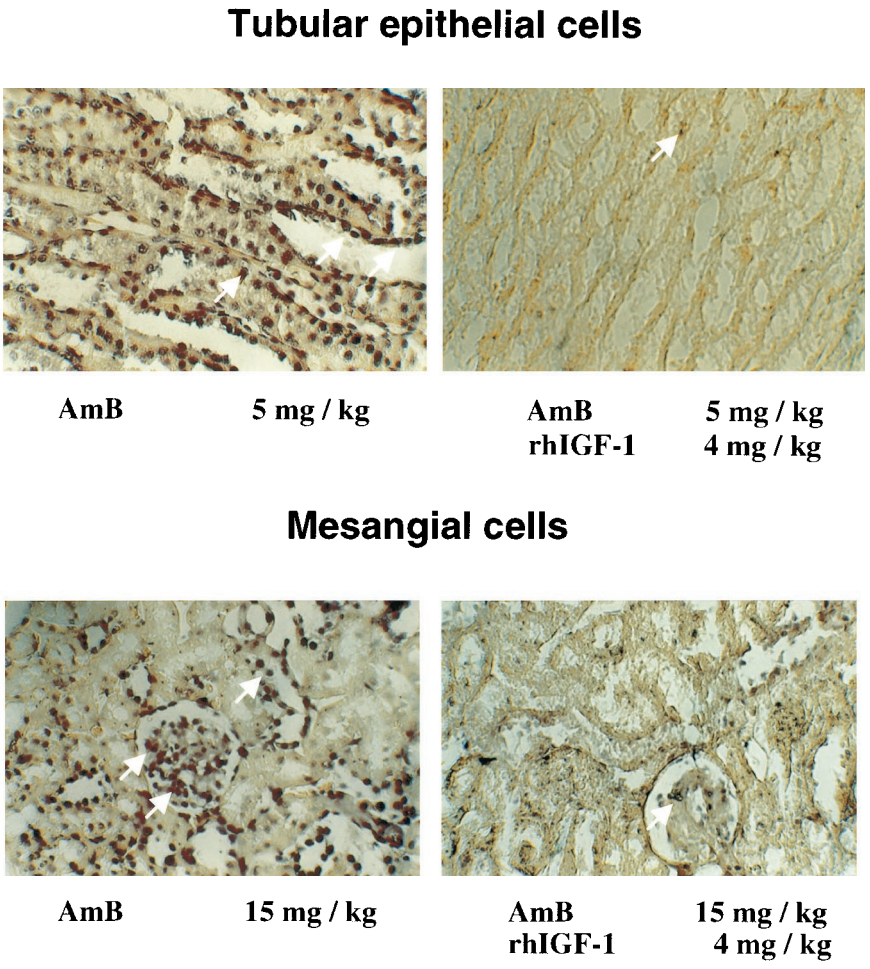

FIG. 2. Photomicrographs of renal tissue sections from Sprague-Dawley rats. Apoptotic cells were detected immunhistochemically by in situ end labeling of DNA strand breaks (TUNEL assay). All dark-stained cells are apoptotic. White arrows indicate apoptotic cells. Tubular epithelial and mesangial cells from rats treated with 5 or 15 mg of AmB/kg gave AI values of 43% ± 4% and 25% ± 1%, respectively (left panels; see also Table 3). Concomitant application of AmB and 4 mg of rhIGF-1 per kg resulted in a significant decrease of the AI in both cell types (right panels).

icant increase of apoptosis within the mesangium. Strikingly, the number of apoptotic cells in kidneys correlated tightly with the degree of hypokalemia, decreased weight gain, loss of renal concentrating ability, and dehydration. We propose here that excess apoptosis accounts for the inability of host tubular epithelial cells to effectively remodel cell injury and thereby plays a role in AmB-induced hypokalemia and polyuria. Other nephrotoxic agents, e.g., cyclosporine (31) and gentamicin (11, 29), lead to a similar distribution of apoptosis within the rat kidney compared to AmB. However, their spectrum of clinical side effects differs. It is conceivable that apoptosis is a common endpoint of toxic renal injury but that the preceding drug-specific gene alterations determine the spectrum of clinical side effects (12, 13, 29, 37).

Furthermore, we found that rhIGF-1 prevented apoptosis in the kidney of animals treated with low and medium doses of AmB and significantly reduced it in rats treated with a high dose of AmB. Moreover, rhIGF-1 abbrogated AmB-induced clinical side effects in all treatment groups.

Although apoptosis is physiologic, its excess could be of pathogenic importance. Excess apoptosis leading to renal impairment has been proposed by Savill (36). It is well known that renal tissue can undergo repair and remodeling when injured (1). However, the loss of cellularity by excess apoptosis may prevent the ability of the kidney to effectively remodel and repair tissue in areas of injury. Therefore, one might wish to prevent renal cell apoptosis as an approach to broadening the therapeutic range of nephrotoxic agents.

The mechanism by which apoptosis induces toxicity secondary to renal injury remains unclear. Subcellular cascades leading to apoptosis can be orchestrated by up- and downregulation of a multitude of genes which encode cytokines, such as tumor necrosis factor (7). Thus, it is conceivable that the clinical side effects are directly related to the action of cytokines.

In conclusion, the present study is the first report to provide evidence that apoptosis is involved in AmB-induced renal injury in a dose-dependent fashion and that the incidence of apoptosis correlates tightly with clinical symptoms of its nephrotoxicity. Furthermore, we could demonstrate that rhIGF-1 not only prevents apoptosis in AmB-treated renal tissue culture cell lines but also abrogates AmB-mediated clinical side effects in the rat model.

ACKNOWLEDGMENTS

We are grateful for the support from the Department of Pediatrics, State University of New York at Stony Brook. We thank R. N. Fine for critical discussion. rhIGF-1 was kindly provided by Genentech, Inc. We thank Diane Trepani for excellent technical assistance. We also thank R. Busch, Department of Statistics, Technical University of Munich, for the data analysis.

H.R. was supported by the "AIDS-Stipendienprogramm" from the Bundesministerium für Bildung, Wissenschaft, Forschung, und Technologie of Germany.

REFERENCES

1. **Abbate, M., and G. Remuzzi.** 1996. Acceleration of recovery in acute renal failure: from cellular mechanisms of tubular repair to innovative targeted therapies. Renal Fail. **18:**377–388.
2. **Aron, D. C., J. L. Rosenzweig, and H. E. Abboud.** 1989. Synthesis and binding of insulin-like growth factor I by human glomerular mesangial cells. J. Clin. Endocrinol. Metab. **68:**585–591.
3. **Baker, N. L., V. C. Russo, O. Bernard, A. J. D'Ercole, and G. A. Werther.** 1999. Interactions between bcl-2 and the IGF system control apoptosis in the developing mouse brain. Brain Res. Dev. Brain Res. **118:**109–118.
4. **Bolard, J.** 1986. How do the polyene macrolide antibiotics affect the cellular membrane properties? Biochem. Biophys. Acta **864:**257–304.
5. **Brajtburg J., W. G. Powderly, G. S. Kobayashi, and G. Medoff.** 1990. Amphotericin B: current understanding of mechanism of action. Antimicrob. Agents Chemother. **34:**183–188.
6. **Cheng, J. T., R. T. Witty, R. R. Robinson, and W. E. Yarger.** 1982. Amphotericin B nephrotoxicity: increased renal resistance and tubule permeability. Kidney Int. **22:**626–633.
7. **Chia, J. K., and E. J. McManus.** 1990. In vitro tumor necrosis factor induction assay for analysis of febrile toxicity associated with amphotericin B preparations. Antimicrob. Agents Chemother. **34:**906–908.
8. **Collette, N., P. van der Auwera, A. P. Lopez, C. Heyman, and F. Meunier.** 1989. Tissue concentration and bioactivity of amphotericin B in cancer patients treated with amphotericin B-deoxycholate. Antimicrob. Agents Chemother. **33:**362–368.
9. **Conti, F. G., L. J. Striker, S. J. Elliot, D. Andreani, and G. E. Striker.** 1988. Synthesis and release of insulinlike growth factor I by mesangial cells in culture. Am. J. Physiol. **255:**1214–1219.
10. **Delaney, C. L., H. L. Cheng, and E. L. Feldman.** 1999. Insulin-like growth factor-I prevents caspase-mediated apoptosis in Schwann cells. J. Neurobiol. **41:**540–548.
11. **El Mouedden, M., G. Laurent, M. P. Mingeot-Leclercq, and P. M. Tulkens.** 2000. Gentamicin-induced apoptosis in renal cell lines and embryonic fibroblasts. Toxicol. Sci. **56:**229–239.
12. **Esposito, C., A. Fornoni, F. Cornacchia, N. Bellotti, G. Fasoli, A. Foschi, I. Mazzucchelli, T. Mazzullo, L. Semeraro, and A. Dal Canton.** 2000. Cyclosporine induces different responses in human epithelial, endothelial and fibroblast cell cultures. Kidney Int. **58:**123–130.
13. **Fornoni, A., O. Lenz, I. Tack, M. Potier, S. J. Elliot, L. J. Striker, and O. Striker.** 2000. Matrix accumulation in mesangial cells exposed to cyclosporine A requires a permissive genetic background. Transplantation **70:**587–593.
14. **Gavrieli, Y., Y. Sherman, and S. A. Ben-Sasson.** 1992. Identification of programmed cell death in situ via specific labeling of nuclear DNA fragmentation. J. Cell Biol. **119:**493–501.
15. **Gouge, T. H., and V. T. Andriole.** 1971. An experimental model of amphotericin B nephrotoxicity with renal tubular acidosis. J. Lab. Clin. Med. **78:**73–81.
16. **Hay, R. J.** 1991. Overview of the treatment of disseminated fungal infections. Antimicrob. Agents Chemother. **28:**17–25.
17. **Hetts, S. W.** 1998. To die or not to die: an overview of apoptosis and its role in disease. JAMA **279:**300–307.
18. **Hirschberg, R., and H. Ding.** 1998. Mechanisms of insulin growth factor-I-induced accelerated recovery in experimental acute renal failure. Miner. Electrolyte Metab. **24:**211–219.
19. **Joly, V., L. Saint-Julien, C. Carbon, and P. Yeni.** 1990. Interactions of free and liposomal amphotericin B with renal proximal tubular cells in primary culture. J. Pharmacol. Exp. Ther. **255:**17–22.
20. **Kavlock, R. J., B. F. Rehnberg, and E. H. Rogers.** 1985. Amphotericin B- and folic acid-induced nephropathies in developing rats. Toxicol. Appl. Pharmacol. **81:**407–415.
21. **LeBrun, M., L. Grenier, P. Gourde, M. G. Bergeron, G. Labrecque, and D. Beauchamp.** 1996. Nephrotoxicity of amphotericin B in rats: effects of the time of administration. Life Sci. **58:**869–876.
22. **Lieberthal, W., and J. S. Levine.** 1996. Mechanisms of apoptosis and its potential role in renal tubular epithelial cell injury. Am. J. Physiol. **271:**477–488.
23. **Lin, J. J., A. V. Cybulsky, P. R. Goodyer, R. N. Fine, and F. J. Kaskel.** 1995. Insulin-like growth factor-I enhances epidermal growth factor receptor activation and renal tubular cell regeneration in postischemic acute renal failure. J. Lab. Clin. Med. **125:**724–733.
24. **Maestri, M., D. C. Dafoe, G. A. Adams, A. Gaspari, F. Luzzana, F. Innocente, J. Rademacher, P. Dionigi, A. Barbieri, F. Zonta, A. Zonta, and R. Rabkin.** 1997. Insulin-like growth factor-I ameliorates delayed kidney graft function and the acute nephrotoxic effecs of cyclosporine. Transplantation **64:**185–190.
25. **Marodi, L.** 1997. Local and systemic host defense mechanism against *Candida*: immunopathology of candidal infections. Pediatr. Infect. Dis. J. **16:**795–801.
26. **Mason, J. L., P. Ye, K. Suzuki, A. J. D'Ercole, and G. K. Matsushima.** 2000. Insulin-like growth factor-I inhibits mature oligodendrocytes apoptosis during primary demyelinisation. J. Neurosci. **20:**5703–5708.
27. **Miller, S. B., D. R. Martin, J. Kissane, and M. R. Hammerman.** 1994. Rat models for clinical use of insulin-like growth factor I in acute renal failure. Am. J. Physiol. **266:**949–956.
28. **Mockridge, J. W., E. C. Benton, L. V. Andreeva, D. S. Latchman, M. S. Marber, and R. J. Heads.** 2000. IGF-I regulates cardiac fibroblast apoptosis induced by osmotic stress. Biochem. Biophys. Res. Commun. **273:**322–327.
29. **Nouwen, E. J., W. A. Verstrepen, N. Buyssens, M. Q. Zhu, and M. E. de Broe.** 1994. Hyperplasia, hypertrophy, and phenotypic alterations in the distal tubule after acute proximal injury in the rat. Lab. Investig. **70:**479–493.
30. **O'Connor, R., A. Kauffmann-Zeh, Y. Liu, S. Lehar, G. I. Evan, R. Baserga, and W. A. Blätter.** 1997. Identification of domains of the insulin-like growth factor I receptor that are required for protection from apoptosis. Mol. Cell. Biol. **17:**427–435.
31. **Ortiz, A., C. Lorz, M. Catalan, A. Ortiz, S. Coca, and J. Egido.** 1998. Cyclosporine A induces apoptosis in murine tubular epithelial cells: role of caspases. Kidney Int. **68:**25–29.
32. **Paller, M. S.** 1990. Drug-induced nephropathies. Med. Clin. North Am. **74:**909–917.
33. **Parrizas, M., and D. LeRoith.** 1997. Insulin-like growth factor I inhibition of apoptosis is associated with increased expression of the local bcl-xL gene product. Endocrinology **138:**1355–1358.
34. **Price, G. J., J. L. Berka, S. R. Edmondson, G. A. Werther, and L. A. Bach.** 1995. Localization of mRNAs for insulin-like growth factor binding protein 1 to 6 in the rat kidney. Kidney Int. **48:**402–411.
35. **Ryu, B. R., H. W. Ko, I. Jou, J. S. Noh, and B. J. Gwag.** 1999. Phosphatidylinositol 3-kinase mediated regulation of neuronal apoptosis and necrosis by insulin and IGF-I. J. Neurobiol. **39:**536–546.
36. **Savill, J.** 1994. Apoptosis and the kidney. J. Am. Soc. Nephrol. **5:**12–21.
37. **Shihab, F. S., T. F. Andoh, A. M. Tanner, H. Yi, and W. M. Bennett.** 1999. Expression of apoptosis regulatory genes in chronic cyclosporine A nephrotoxicity favors apoptosis. Kidney Int. **56:**2147–2159.
38. **Steller, H.** 1995. Mechanisms and genes of cellular suicide. Science **267:**1445–1449.
39. **Thornberry, N. A., and Y. Lazebnik.** 1998. Caspases: enemies within. Science **281:**1312–1316.
40. **Weldon, M. W., and M. E. Schultz.** 1974. Renal ultrastructure after amphotericin B. Pathology **6:**191–200.
41. **Zager, R. A., C. R. Bredl, and B. A. Schimpf.** 1992. Direct amphotericin B-mediated tubular toxicity: assessments of selected cytoprotective agents. Kidney Int. **41:**1588–1594.
42. **Zager, R. A.** 1997. Pathogenetic mechanisms in nephrotoxic acute renal failure. Semin. Nephrol. **17:**3–14.